

Article

Dynamic Adsorption of Sulfamethoxazole from Aqueous Solution by Lignite Activated Coke

Haiyan Li ^{1,2}, Juan He ¹, Kaiyu Chen ¹, Zhou Shi ¹, Mengnan Li ¹, Pengpeng Guo ¹ and Liyuan Wu ^{1,2,*}

¹ Beijing Engineering Research Center of Sustainable Urban Sewage System Construction and Risk Control, Beijing University of Civil Engineering and Architecture, Beijing 100044, China; Lihaiyan@bucea.edu.cn (H.L.); louyounan@163.com (J.H.); Chenkaiyuxiao@163.com (K.C.); shizhou2016@163.com (Z.S.); lmn970109@163.com (M.L.); gzpjustice@163.com (P.G.)

² Beijing Advanced Innovation Center for Future Urban Design, Beijing 100044, China

* Correspondence: wuliyuan@bucea.edu.cn; Tel.: +86-010-68-322-452

Received: 2 March 2020; Accepted: 7 April 2020; Published: 10 April 2020



Abstract: In this paper, lignite activated coke was used as adsorbent for dynamic column adsorption experiments to remove sulfamethoxazole from aqueous solution. The effects of column height, flow rate, initial concentration, pH and humic acids concentration on the dynamic adsorption penetration curve and mass transfer zone length were investigated. Results showed penetration time would be prolonged significantly by increasing column height, while inhibited by the increasement of initial concentration and flow rate. Thomas and Yoon-Nelson model and the Adams-Bohart model were used to elucidate the adsorption mechanism, high coefficients of $R^2 > 0.95$ were obtained in Thomas model for most of the adsorption entries, which revealed that the adsorption rate could probably be dominated by mass transfer at the interface. The average change rates of mass transfer zone length to the changes of each parameters, such as initial concentration, the column height, the flow rate and pH, were 0.0003, 0.6474, 0.0076, 0.0073 and 0.0191 respectively, revealed that column height may play a vital role in dynamic column adsorption efficiency. These findings suggested that lignite activated coke can effectively remove sulfamethoxazole contaminants from wastewater in practice.

Keywords: lignite activated coke; sulfamethoxazole; dynamic; adsorption; penetration curve; modeling

1. Introduction

Pharmaceuticals and personal care products (PPCPs) have become emerging pollutants due to the large amount of human consumption and usage [1–4]. Relating to the properties of high polarity and low volatility, PPCPs tend to be distributed and migrated to the environment through water phase transfer and food chain diffusions [5,6]. At present, many PPCPs pollutants have been detected in surface water, groundwater, drinking water and sewage, in the level of ng/L to $\mu\text{g/L}$, which will have potentially toxicological effects on the aquatic organisms [6]. Besides, the accumulation of these chemicals through the food chain may be harmful to human health [7]. Thus, it is necessary to develop effective treatment options to reduce their release into the environment. Up to now, various methods to remove PPCPs from wastewater have been developed, including photocatalysis [8,9], advanced oxidation [10,11], electrocatalysis [12,13], adsorption [14,15] and so on.

Sulfamethoxazole is a typical broad-spectrum antibiotic, which has been used in large quantities due to its inhibiting ability towards bacteria sensitivity [16]. Many methods, such as photocatalysis, advanced and fenton oxidation technology can effectively removal sulfamethoxazole from aqueous solution but the complicated operations, high cost and safety concerns has limited their application [14,16–20]. Therefore, the adsorption method is often used in industrial wastewater treatment due to the convenient operation

in the advanced treatment stage. Different materials, such as carbon materials [21–23], composite metal materials [24–26], graphene oxide [27,28], metal-organic frameworks (MOFs) [29], resins [30] and so on have been reported with considerable adsorption capacity for sulfamethoxazole. However, considering practical use for wastewater treatment, economic materials with good mechanical strength, high adsorption capacity and fast removal efficiency are still being researched for sulfamethoxazole removal from aqueous solution. Lignite activated cokes (abbreviated as LACs), which are produced from carbonaceous materials, have been widely used in water treatment in recent years due to their benefits of high mechanical strength, cheapness, macroporous and mesoporous structures and oxygen-containing organic functional groups [31–33]. These have attracted extensive attention to LACs in the field of wastewater treatment in recent years. In this paper, the dynamic adsorption behavior of LACs towards sulfamethoxazole in aqueous solution was investigated.

The effects of column height, initial concentration, flow rate, humic acids and pH on dynamic adsorption behavior were comparatively analyzed to determine the optimized condition for dynamic adsorption. The models of Thomas, Yoon-Nelson and Adams-Bohart were fitted to experiment data and the Thomas has high correlation coefficients. The homogeneous surface diffusion model (HDSM) was fitted to a breakthrough curve and obtained the surface diffusion constant.

2. Materials and Methods

2.1. Materials, Reagents and Tests

Commercial LACs (1–2 mm) with a specific surface area of $790 \text{ m}^2 \text{ g}^{-1}$ was obtained from Beijing Guodian Futong Technology Co., Ltd. (Beijing, China) and purified as follows [34]. Two grams of LACs was poured into a beaker containing 500 mL deionized water, boiled for 30 min, washed with deionized water for several times and dried at $105 \text{ }^\circ\text{C}$ for 24 h. Sulfamethoxazole (analytical grade) was purchased from Macleans Corporation (>99%, Shanghai, China). Humic acids, NaOH, HCl and NaCl were purchased from Sinopharm (Shanghai, China). These chemicals were used directly without purification.

The concentration of sulfamethoxazole in aqueous solution was measured by Acquity UPLC-H, with a C18 analytical column ($1.7 \mu\text{m} \times 2.1 \text{ mm} \times 50 \text{ mm}$) (ACQUITYUPLC, Waters, Milford, MA, USA), mobile phase (0.01% acetic acid solution: methanol = 30:70), flow rate (0.35 mL/min), column temperature 303 K, $\lambda = 265 \text{ nm}$ and the retention time was 0.7 min.

2.2. Equipment and Conditions of Column Experiments

2.2.1. Column Experimental Device

All the dynamic adsorption experiments were operated in a series of abbreviated wet packing glass columns, with an inner diameter of 2.5 cm, as shown in Figure 1. For each column, 0.5 cm glass beads, 3 cm LACs (with particle size of 100 mesh) and 0.5 cm glass beads were successively filled into the column, pressed tightly and uniformly. Prior to the experiment, the deionized water was inflow into the column completely to exclude the air in the porosity of cokes until the pH of effluent arrived neutral, thus to maintain the stability of pore structures inside the adsorption column. ρ_0 is the loading density of activated coke in the column (g/cm^3). The aqueous solution of sulfamethoxazole was loaded into the column through the inlet at the bottom of the reactor and suctioned by a peristaltic pump under a steady flow. Samples were taken from the outlet at the fixed time intervals. Except for the column height experiment, the other experiment samples were received from outlets located at a column height of 3 cm. The concentrations of sulfamethoxazole in the sampling solution were tested by UPLC with a retention time of 0.7 min. With this device, the dynamic adsorption behaviors under different operation factors such as pollutant concentration, flow rate, pH and packing column height were investigated.

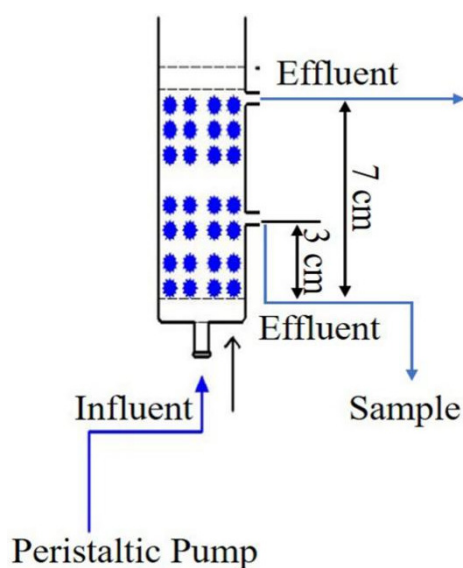


Figure 1. The experimental device of column adsorption.

2.2.2. Column Experiments

For the column adsorption experiments, the sulfamethoxazole solution (ion strength of 10 mmol/L NaCl) was pumped into the column from bottom to top by a peristaltic pump. The effect of different initial sulfamethoxazole concentrations (35 mg/L “vs.” 75 mg/L), column heights (3 cm “vs.” 7 cm), inlet flow rates (3 mL/min “vs.” 5 mL/min), solution pH (4, 6.5 and 8) and humic acids concentration (0, 0.1, 1 and 10 mg/L) on breakthrough curves were studied.

In the pH effect experiments, sulfamethoxazole solutions (35 mg/L) with initial pH values of 4, 6.5 and 8 were prepared, respectively. Aqueous HCl (0.10 mol/L) or NaOH (0.10 mol/L) were used to adjust the pH. Two outlets were designed in the column with a height of 3 cm and 7 cm respectively. In the column experiments with column height of 7 cm, the lower outlet at 3 cm was sealed. At certain intervals, in eluate, the concentration of the sulfamethoxazole was determined.

Herein, the time with the sampling concentration reaching 10% and 95% of the initial concentration were defined as the adsorption penetration point (t_b , min) and the adsorption penetration end time (t_e , min). The length (H , cm) of the mass transfer zone of the adsorption column was calculated based on the adsorption penetration point time t_b and the adsorption penetration end time t_e as follows (1):

$$H = \frac{C_0 Q}{q \rho_0 A} (t_e - t_b) \quad (1)$$

Q represents the flow rate (mL/min); C_0 is the inlet sulfamethoxazole concentration (mg/L); q is the amount adsorption capacity (mg/g) of sulfamethoxazole by unit activated coke; ρ_0 is the loading density of activated coke in the column (g/cm^3). A is the cross-sectional area of the adsorption column (cm^2).

The adsorption capacity q is calculated according to Equation (2) [15,35]:

$$q = (C_0 - C_e) \frac{V}{M} \quad (2)$$

Among them, C_0 and C_e were determined by UPLC with a retention time of 0.7 min. q is the dynamic saturated adsorption amount (mg/g); C_0 is the inlet concentration of sulfamethoxazole (mg/L); C_e is the outlet concentration of sulfamethoxazole; V (L) is the solution volume; M is the mass weight of the adsorbents (g).

3. Results and Discussion

3.1. Adsorption Performance of Sulfamethoxazole on LACs

3.1.1. Effect of Initial Concentration

The breakthrough curves of sulfamethoxazole adsorption performance on LACs were described from a series of column adsorption entries to evaluate the enrichment capacity of LACs. At a fixed column height of 3 cm, a flow rate of 3 mL/min, pH 6.5, column adsorption under initial sulfamethoxazole concentration of 35 mg/L and 70 mg/L were comparatively studied. The samples were received from the outlet located at a column height of 3 cm. As shown in Figure 2 and Table 1, with the increase of initial concentration, the bed volume decreased from 210 to 120 cm³.

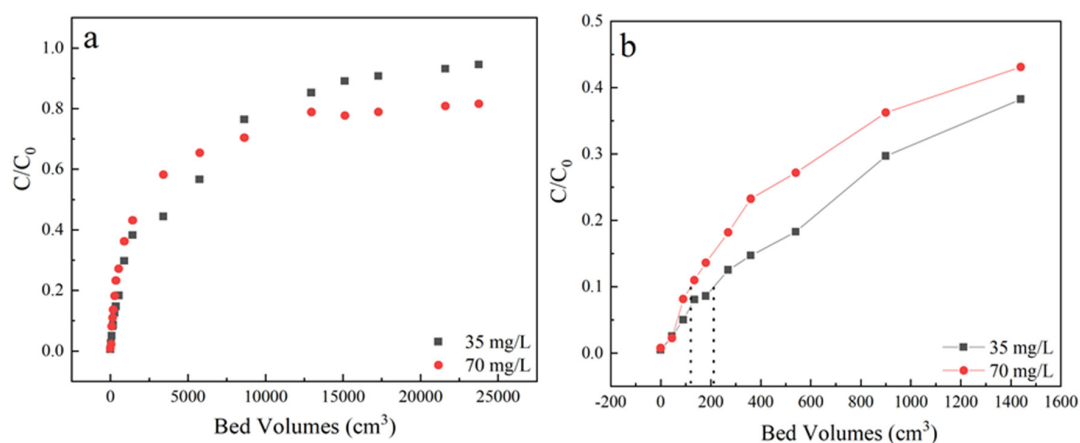


Figure 2. (a) The effect of different concentration of sulfamethoxazole adsorption breakthrough curves; (b) Partially enlarged screening from 0 to 1600 bed volume. Experiment condition: flow rate of 3 mL/min, column height of 3 cm, pH 6.5, sulfamethoxazole concentration of 35 and 70 mg/L, respectively.

The time required to reach 50% of initial concentration was obviously extended from 12 h to 25 h, which may be due to that high initial concentration, increased the sulfamethoxazole concentration difference between activated coke and solutions, making the breakthrough curve slope steeper [36]. On the other hand, it was clear that the time required to reach saturation decreased with the increasing of the initial concentration, as the diffusion rate is controlled by the concentration gradient. As the initial concentration of pollutants increased, the bed utilization rate decreased. Besides, the adsorption penetration end time in the system of 70 mg/L could not be reached, the C/C_0 after 140 h was close to 0.8 and arrived in equilibrium, which indicated that a certain retention effect may exist in the liquid flow system of the adsorption column under high sulfamethoxazole initial concentration.

3.1.2. Effect of Column Height

At a fixed flow rate of 3 mL/min, initial sulfamethoxazole concentration of 35 mg/L and pH 6.5, column adsorption under different column heights of 3 cm and 7 cm were studied to assess the effect of column height on the dynamic adsorption. From Figure 3 and Table 1, it was observed that column height had a positive relationship with the bed adsorption capacity. Under a high column height of 7 cm, the bed volume could be extended remarkably from 210 to 395 cm³. Besides, the curve slope became smooth under a higher column length. Undoubtedly, the amounts of LACs increased, the adsorption capacity could be enhanced, and high breakthrough time gave better intraparticle diffusion phenomena. Some references have mentioned that carbon-based materials with high mesopores, large pore volumes and medium specific surface area have the best adsorption effect on sulfamethoxazole [32,37]. LACs contained a number of macropore and mesoporous structures, attributed not only to the increasing of the specific surface area but also enhancing the sulfamethoxazole removal by increasing the

spread of contaminant and a capacity of the sorbent material [34]. Moreover, LACs contain many oxygen-containing functional groups, such as phenolic groups, which could provide abundant binding sites for sulfamethoxazole through hydrogen-bonding interactions. The curves shape noted for 3 cm was more upright than 7 cm, this might be because a larger mass transfer region has formed in the longer column, which retarded the arrival of penetration time.

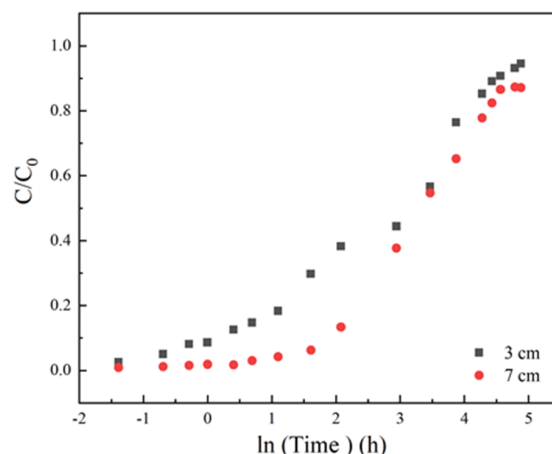


Figure 3. The adsorption effect of different column height on breakthrough curves, Experiment condition: sulfamethoxazole concentration of 35 mg/L, flow rate of 3 mL/min, pH 6.5, column height 3, 7 cm, respectively.

3.1.3. Effect of Flow Rate

Flow rate is an important parameter for industrial-scale wastewater treatment. The samples were received from the outlet located at a column height of 3 cm, sulfamethoxazole concentration of 35 mg/L at pH 6.5, the adsorption flow rates were varied from 3 mL/min to 5 mL/min, the corresponding dynamic adsorption breakthrough curves were compared in Figure 4 and Table 1. It could be found that the steepness increased with the flow rate, resulting in an earlier breakthrough point volume under 5 mL/min.

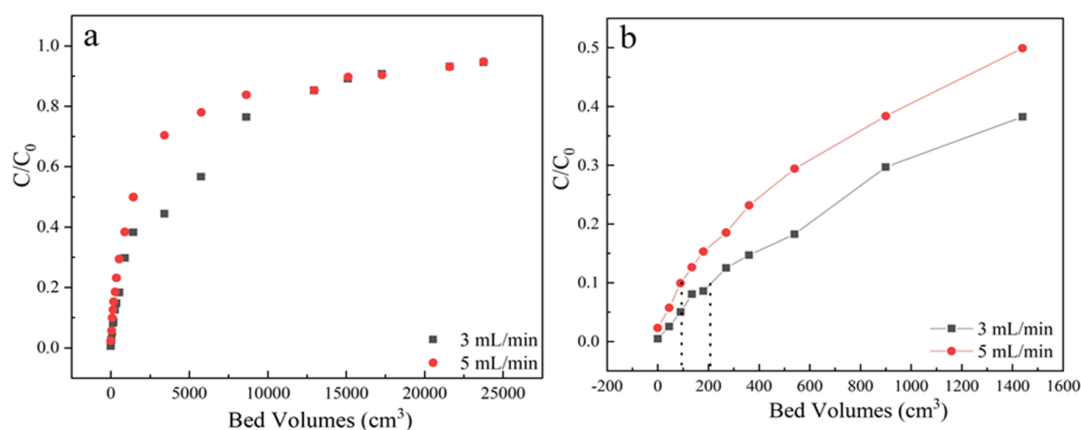


Figure 4. (a) The adsorption effect of different flow rate on breakthrough curves; (b) Partially enlarged screening from 0 to 1600 bed volume. Experiment condition: sulfamethoxazole concentration of 35 mg/L, pH 6.5, column height of 3 cm, flow rate of 3, 5 mL/min, respectively.

This is because that low flow rate can offer enough time for intra-particle diffusion of pollutants at the interface of adsorbents as well as a binding interaction between sulfamethoxazole and functional groups of LACs. And the flow rate will affect the external film diffusion but not the surface diffusion. Contrarily, high flow rate of 5 mL/min could easily cause the decrease of mass transfer resistance, then

the breakpoint time and saturation were quickly reached. Besides, fast flow rate would also reduce the utilization efficiency of the fixed bed before reached to saturation.

Table 1. Comparative data of penetration curves of dynamic coke adsorption sulfamethoxazole dynamic column experiments.

Concentration (mg/L)	Flow Rate (mL/min)	Column Height (cm)	pH	Humic Acids (mg/L)	10% Breakthrough Volume (cm ³)	95% Breakthrough Volume (cm ³)
35	3	3	6.5	0	210	23745
70	3	3	6.5	0	110	20820
35	3	3	6.5	0	210	23745
35	5	3	6.5	0	98	24000
35	3	3	6.5	0	210	23745
35	3	7	6.5	0	395	30000
35	3	3	4	0	15	20700
35	3	3	6.5	0	210	23745
35	3	3	8	0	115	12636
35	3	3	6.5	0	210	23745
35	3	3	6.5	0.1	680	-
35	3	3	6.5	1	20	17220
35	3	3	6.5	10	250	26190

3.1.4. Effect of pH

In the actual wastewater treatment process, pH factor will affect the effectiveness of the adsorbent to remove pollutants. So, it is necessary to consider the pH effect on wastewater treatment. Herein, effect of pH was executed at 4, 6.5 and 8 under the condition of 35 mg/L sulfamethoxazole concentration, 3 mL/min flow rate and the samples were received from the outlets, located at a column height of 3 cm.

As shown in Figure 5 and Table 1, the best adsorption performance was obtained at pH 6.5. The pH_{pzc} of activated coke was 6.5 and the pK_a of sulfamethoxazole was 5 [38]. At pH 4, electrostatic interaction contributes to the major adsorption mechanism due to the negatively charged sulfamethoxazole species and the positively charged surface of LACs. At pH 6.5, the sulfamethoxazole species were negatively charged while the surface of LACs was nearly uncharged, the hydrogen-bonding interaction played an important role during adsorption because the phenolic groups of LACs and the N, O atoms of sulfamethoxazole species. Similar observations were also reported in diclofenac sodium adsorption on oxidized activated carbon [39]. At pH 8.0, the sulfamethoxazole species and the surface of LACs were both negatively charged, the electrostatic repulsion could inhibit the sulfamethoxazole adsorption, thus a lowered penetration time was obtained.

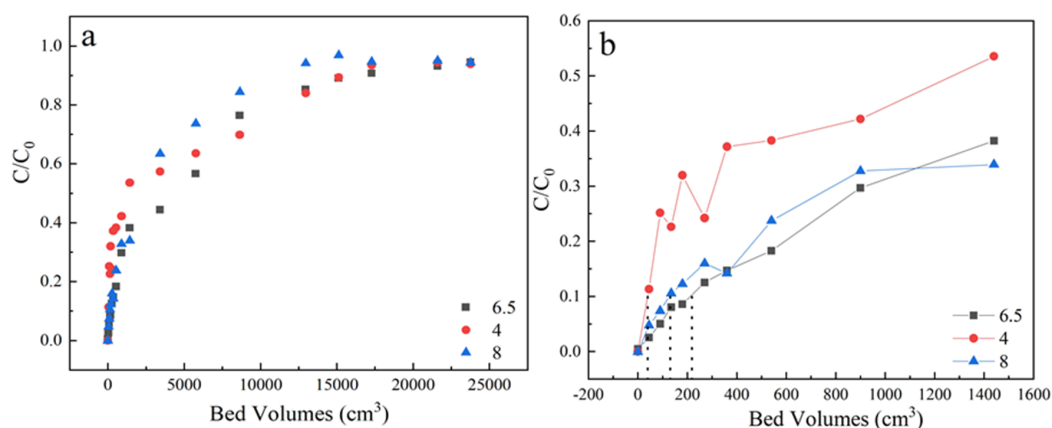


Figure 5. (a) The adsorption effect of different pH on breakthrough curves, (b) Partially enlarged screening from 0 to 1600 bed volume. Experiment condition: flow rate of 3 mL/min, column height of 3 cm, sulfamethoxazole concentration of 35 mg/L, pH 4, 6.5, 8 respectively.

3.1.5. Effect of Humic Acids

The effect of humic acids was executed at 0, 0.1, 1 and 10 mg/L under the condition of 35 mg/L sulfamethoxazole concentration, 3 mL/min flow rate and the samples were received from the outlets, located at a column height of 3 cm. As shown in Figure 6 and Table 1, the penetration time increase slowly during 0–0.1 mg/L and decreased deeply when organic concentration increased to 1 mg/L. When increasing the concentration of organic matter to 10 mg/L, the adsorption ability increased a little. The slopes of penetration curves under different humic acids concentration follows in the order of $1 > 0 > 10 > 0.1$ mg/L. These results illustrated that the existence of humic acids would affect the dynamic adsorption behavior.

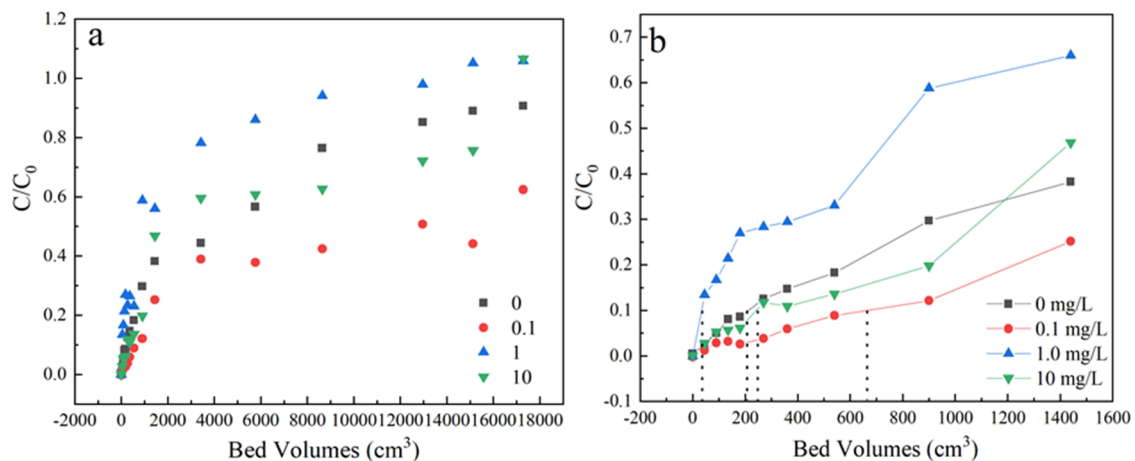


Figure 6. (a) The adsorption effect of different concentration of human acids on breakthrough curves, (b) Partially enlarged screening from 0 to 1600 bed volume. Experiment condition: flow rate of 3 mL/min, column height of 3 cm, sulfamethoxazole concentration of 35 mg/L, pH 6.5, humic acids concentration = 0, 0.1, 1, 10 mg/L, respectively.

3.2. Breakthrough Curves Models Analysis

To elucidate the adsorption mechanism of sulfamethoxazole on LACs, the Thomas model, Yoon-Nelson and Adams-Bohart model were used to predict the performance and parameters of the fixed-bed column. The Thomas model is derived depending upon second-order kinetics and assumed that the sorption is dominated by mass transfer at the interface not the chemical reaction [40]. The mathematical form is as follows:

$$\ln\left(\frac{C_0}{C_t} - 1\right) = k_T q_e \frac{m}{Q} - k_T C_0 t \quad (3)$$

C_0 and C_t (mg/L) are the concentration of solution in the inlet and outlet at time t (min), k_T (mL/(min·mg)) is the Thomas rate constant, Q (mL/min) is the flow rate, q_e (mg/g) is the maximum sorption capacity, m (g) is the mass of activated coke.

The Yoon-Nelson model assumes that the rate of decreasing in the probability of adsorption for each adsorbate molecule is directly proportional to adsorbate breakthrough probability and adsorbate adsorption probability [41]. The Yoon-Nelson does not rely on the physical factors bed and adsorbate characteristics [42].

$$\ln\left(\frac{C_t}{C_0 - C_t}\right) = k_Y t - k_Y \tau \quad (4)$$

C_0 and C_t (mg/L) are the concentrations of solution in the inlet and outlet at time t (min), k_Y (1/min) is the Yoon-Nelson rate constant, τ (min) is the time to reach 50% of sulfamethoxazole breakthrough.

Except for the linearized Equation, Thomas and Yoon-Nelson models are equivalent in terms of mathematical form as described in Reference [43]:

$$Y = \frac{1}{(1 + \exp(-kt + b))} \quad (5)$$

The Adams-Bohart model was based on the surface reaction theory, applied to account for the initial part of the breakthrough curve. The Adams-Bohart model and its mathematical form are as follows [40]:

$$\ln\left(\frac{C_t}{C_0}\right) = K_A C_0 t - N_0 h \frac{k_A}{v} \quad (6)$$

$$Y = \exp(kt + b). \quad (7)$$

C_0 and C_t (mg/L) are the concentration of solution in the inlet and outlet at time t (min), k_A (L/(min·g)) is the Yoon-Nelson rate constant, N_0 (g/L) is the sorption capacity of the adsorbent per unit volume of the bed, h (mm) is the column height, v (mm/min) is the flow rate. The analysis of C_e/C_0 and t at different experimental conditions was performed.

As shown in Figure 7 and Table 2, high correlation coefficients $R^2 > 0.95$ were obtained in the Thomas model for all the adsorption entries (except for the column height of 7 cm), For the Yoon-Nelson model, adsorption entries under low experiment parameters (such as 35 mg/L sulfamethoxazole concentration, 3 mL/min flow rate and 7 cm column height) fitted better than the higher ones, with correlation coefficients $R^2 > 0.95$. While a low R^2 value obtained in the Adams-Bohart model indicated worse fitting results of experiment data. These calculation results demonstrated that the adsorption rate could be probably dominated by mass transfer at the interface, due to the microporous and mesoporous structure characteristics of LACs, similar conclusions were also reported in diclofenac sodium adsorption on LACs [34]. The value of the model's parameters, such as k_T , k_Y , q_e and τ depends on experimental conditions such as flow rate, initial concentration and column height. The initial concentration of sulfamethoxazole could obviously affect the maximum sorption capacity, q_e , long column height of LACs may inhibit the adsorption rate due to the sharply decreasing k_T in 7 cm column height entry.

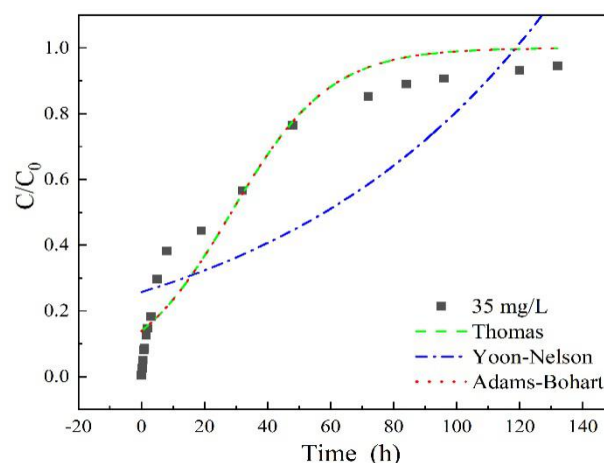


Figure 7. Adsorption breakthrough curves fitted by different models with sulfamethoxazole initial concentration of 35 mg/L, flow rate of 3 mL/min, pH 6.5, column height of 3 cm.

Table 2. The summary of experiment parameters calculated from different models under various experimental conditions.

Models	Initial Concentration (mg/L)		Flow Rate (mL/min)		Column Height (cm)	
	35	70	3	5	3	7
Thomas						
R ²	0.953	0.951	0.953	0.950	0.953	0.93
q _e (mg/g)	3.04	11.56	3.04	4.37	3.04	3.09
k _T (mL/(mg·min))	0.039	0.032	0.039	0.039	0.039	0.010
Yoon-Nelson						
R ²	0.95	0.90	0.953	0.91	0.953	0.93
τ (h)	25	12	25	12	38.7	80
k _Y (1/min)	0.045	0.039	0.045	0.078	0.045	0.038
Adams-Bohart						
R ²	0.72	0.63	0.72	0.63	0.72	0.71
k _A (L/(mg·min))	0.456	0.375	0.456	0.377	0.456	0.54
N ₀ (g/L)	2.6	3.0	2.6	2.5	2.6	2.83

3.3. Homogeneous Surface Diffusion Model (HSDM)

The HSDM model is one of the most widely used dual-resistance diffusion models to predict the fixed bed adsorption process. Through optimizing the fit curve to the experiment breakthrough curve, the surface diffusion coefficient D_s can be obtained [44]. The HSDM was used to evaluate the diffusion coefficient of experiment data. The Equations of the HSDM model are listed as follows [45]. Freundlich isotherm parameters (K , $1/n$) needed in HSDM model by adsorption isotherm were presented in the Supplementary material (Table S1 and Figure S1) [46].

$$\frac{\partial c(z,t)}{\partial t} = D_L \frac{\partial^2 c(z,t)}{\partial Z^2} - D \frac{\partial c(z,t)}{\partial Z} - \frac{3(1-\epsilon)}{\epsilon R} k_f [c(z,t) - c_s(z,t)] \quad (8)$$

The mass balance Equation of particle can be represented as:

$$\frac{\partial q(r,z,t)}{\partial t} = D_s \left[\frac{\partial^2 q(r,z,t)}{\partial r^2} + \frac{2}{r} \frac{\partial q(r,z,t)}{\partial r} \right] \quad (9)$$

The moving phase and particle concentration is correlated with Freundlich Equation:

$$q(r=R,z,t) = KC_s(z,t)^{1/n} \quad (10)$$

The initial and boundary conditions are:

$$\begin{aligned} c(z=0,t>0) &= C_0 \\ \frac{\partial c(z=L,t)}{\partial z} &= 0 \\ \frac{\partial q(r=0,z,t)}{\partial r} &= 0 \\ \rho_p D_s \frac{\partial q(r=R,z,t)}{\partial r} &= k_f [c(z,t) - c_s(z,t)] \end{aligned} \quad (11)$$

The surface diffusion coefficient (D_s) depends on the nature of adsorbents. So, the experimental breakthrough curves at a concentration of 35 mg/L, a flow rate at 3 mL/min, a column height of 3 cm and pH 6.5 conditions were fitted with the HSDM, as shown in Figure 8. The determined surface diffusion coefficient is $2.39 \times 10^{-9} \text{ cm}^2/\text{min}$.

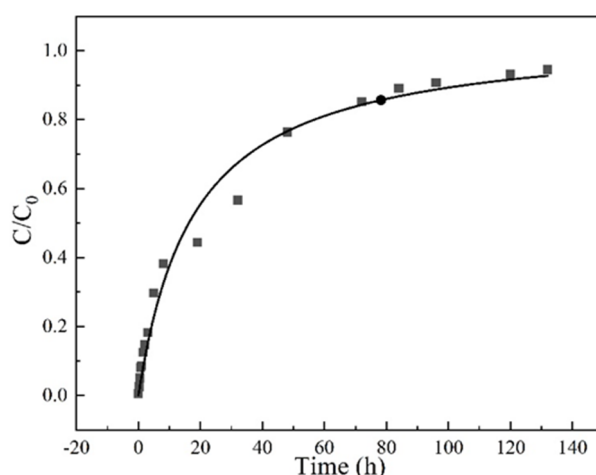


Figure 8. The homogeneous surface diffusion model (HDSM) diffusion model fitted breakthrough curve Experiment condition: sulfamethoxazole concentration of 35 mg/L, flow rate of 3 mL/min, pH 6.5, column height 3 cm.

The sum of square of error (SSE) between the experimental data and the theoretical simulation was used to evaluate the feasibility of the model. As shown in Table 3, the value of SSE is 0.04, demonstrating that the proposed HSDM model can successfully describe the adsorption and diffusion behavior in the fixed bed.

$$SSE = \sum \left[\frac{c_{\text{cal}} - c_{\text{exp}}}{c_0} \right]^2 \quad (12)$$

Table 3. The SSE of HSDM models.

Time (h)	0	0.25	0.5	0.75	1	1.5	2	3	5
C_{cal}	0.00	0.01	0.03	0.04	0.06	0.08	0.11	0.15	0.23
C_{exp}	0.00	0.03	0.05	0.08	0.09	0.13	0.15	0.18	0.30
Time (h)	8	19	32	48	72	84	96	120	132
C_{cal}	0.32	0.54	0.67	0.77	0.84	0.87	0.89	0.92	0.93
C_{exp}	0.38	0.44	0.57	0.76	0.85	0.89	0.91	0.93	0.95
SSE					0.04				

3.4. Evaluation of Factors Effect

In order to investigate the optimized parameters for dynamic adsorption of sulfamethoxazole on LACs, the effects of initial concentration, column height, flow rate, pH and organic matter on the penetration time and the length of the mass transfer zone were compared systematically. As shown in Table 4, the absolute value of average rate ($\Delta t_b/\Delta x$ or $\Delta H/\Delta x$) were calculated from the increments of penetration time (Δt_b), mass transfer zone length (ΔH) for each factor increments (Δx).

The average change rates of the penetration time to the changes of adsorption parameters ($\Delta t_b/\Delta x$), Δx represents initial concentration, column height, flow rate and pH, were 0.86, 98.25, 20, 12.25, respectively. Thus, column height may play a vital role in penetration time. The same results were also gained for $\Delta H/\Delta x$.

The average change rates of the length of the mass transfer zone with respect to the initial concentration, the column height, the flow rate, pH and organic matter were 0.0003, 0.6474, 0.0076, 0.0073 and 0.0191, respectively. Therefore, the change of the initial concentration has the lowest effect on the average rate of change in the length of the mass transfer zone and the column height has the greatest effect on it. These calculations were in accordance with the studies in the above adsorption effects sections.

Table 4. Analysis of each factor on the length of the mass transfer zone of the activated coke adsorption sulfamethoxazole dynamic column experiment.

Factor	Variable X	H	Δx	Δt_b	ΔH	$ \Delta t_b/\Delta x $	$ \Delta H/\Delta x $
Initial sulfamethoxazole concentration	35 mg/L	2.973	35	30	0.009	0.86	0.003
	70 mg/L	2.982					
Column height	3 cm	2.988	4	393	2.59	98.25	0.6474
	7 cm	5.578					
Flow rate	3 mL/min	2.973	2	40	0.015	20	0.0076
	5 mL/min	2.988					
pH	4	3.346	4	61	0.448	12.25	0.0073
	6.5	2.973					
	8	3.421					
Humic acids	0.1 mg/L	3.474	9.9	220	0.189	2.22	0.0191
	1 mg/L	3.333					
	10 mg/L	3.285					

Note: t_b is the penetration time; t_e is the end time of penetration; H is the length of the mass transfer zone; $\Delta x = x_{\max} - x_{\min}$; $\Delta t_b = t_{b\max} - t_{b\min}$; $\Delta H = H_{\max} - H_{\min}$

4. Conclusions

Dynamic column adsorption of sulfamethoxazole by lignite activated coke from aqueous solution were conducted under different initial sulfamethoxazole concentrations, flow rates, column height and pH to investigate the optimized adsorption conditions for wastewater treatment. Results demonstrated that activated coke has high adsorption efficiency for sulfamethoxazole removal from aqueous solution. Increasing the concentration of pollutants and the flow rate will shorten the penetration time, while opposite tendency was found in the column height effect. The best adsorption performance was obtained at pH 6.5 due to the possible hydrogen bonding interaction between sulfamethoxazole species and LACs. The adsorption capacity of activated coke increased by increase in the column height. The Thomas model could best describe the column adsorption behavior with $R^2 > 0.95$ for nearly all adsorption entries. The column height of the activated cokes played a vital role in long penetration time and mass transfer zone.

Supplementary Materials: The following are available online at <http://www.mdpi.com/1996-1944/13/7/1785/s1>, Figure S1: Adsorption isotherms of sulfamethoxazole. Condition: under low initial concentrations of 1~50 mg/L. Adsorbent dosage = 0.5 g/L, pH = 6.5 ± 0.1, [NaCl] = 10 mmol/L, Table S1: Adsorption isotherms parameters.

Author Contributions: Data curation and writing, J.H. and K.C.; Formal analysis, Z.S., M.L. and P.G.; Funding acquisition, L.W.; Methodology, J.H. and K.C.; Software, Z.S., M.L. and P.G.; Writing—original draft, H.L.; Fund supporting and Designing, L.W. All authors have read and agreed to the published version of the manuscript.

Funding: This research was funded by Natural Science Foundation of China, (No. 51678025 & 51978032); Great Wall Scholars Program (CIT&TCD20170313); Youth Top Talents Training Program (CIT&TCD201804052); Science & Technology Foundation of POWERCHINA Co., Ltd (DJ-ZDXM 201619).

Conflicts of Interest: The authors declare no conflict of interest.

References

- Perez-Lemus, N.; Lopez-Serna, R.; Perez-Elvira, S.I.; Barrado, E. Analytical methodologies for the determination of pharmaceuticals and personal care products (PPCPs) in sewage sludge: A critical review. *Anal. Chim. Acta* **2019**, *1083*, 19–40. [[CrossRef](#)] [[PubMed](#)]
- Yang, L.; Zhou, Y.; Shi, B.; Meng, J.; He, B.; Yang, H.; Yoon, S.J. Anthropogenic impacts on the contamination of pharmaceuticals and personal care products (PPCPs) in the coastal environments of the Yellow and Bohai seas. *Environ. Int.* **2020**, *135*, 105306. [[CrossRef](#)] [[PubMed](#)]
- Tarpani, R.R.Z.; Azapagic, A. Life cycle environmental impacts of advanced wastewater treatment techniques for removal of pharmaceuticals and personal care products (PPCPs). *J. Environ. Manag.* **2018**, *215*, 258–272. [[CrossRef](#)] [[PubMed](#)]

4. Liu, M.; Yin, H.; Wu, Q. Occurrence and health risk assessment of pharmaceutical and personal care products (PPCPs) in tap water of Shanghai. *Ecotoxicol. Environ. Saf.* **2019**, *183*, 109497. [[CrossRef](#)]
5. Wang, J.; Chu, L. Irradiation treatment of pharmaceutical and personal care products (PPCPs) in water and wastewater: An overview. *Radiat. Phys. Chem.* **2016**, *125*, 56–64. [[CrossRef](#)]
6. Liu, J.L.; Wong, M.H. Pharmaceuticals and personal care products (PPCPs): A review on environmental contamination in China. *Environ. Int.* **2013**, *59*, 208–224. [[CrossRef](#)]
7. Yang, Y.; Ok, Y.S.; Kim, K.H.; Kwon, E.E.; Tsang, Y.F. Occurrences and removal of pharmaceuticals and personal care products (PPCPs) in drinking water and water/sewage treatment plants: A review. *Sci. Total Environ.* **2017**, *596*, 303–320. [[CrossRef](#)]
8. Khan, M.; Fung, C.S.L.; Kumar, A.; He, J.; Lo, I.M.C. Unravelling mechanistic reasons for differences in performance of different Ti- and Bi-based magnetic photocatalysts in photocatalytic degradation of PPCPs. *Sci. Total Environ.* **2019**, *686*, 878–887. [[CrossRef](#)]
9. Zeng, L.; Li, S.; Li, X.; Li, J.; Fan, S.; Chen, X. Visible-light-driven sonophotocatalysis and peroxydisulfate activation over 3D Urchin-like MoS₂/C nanoparticles for accelerating levofloxacin elimination: Optimization and kinetic study. *Chem. Eng. J.* **2019**, *378*, 122039. [[CrossRef](#)]
10. Alkhouraji, T.S. Advanced oxidation process based on water radiolysis to degrade and mineralize diclofenac in aqueous solutions. *Sci. Total Environ.* **2019**, *688*, 708–717. [[CrossRef](#)]
11. Zhang, T.; Chen, Y.; Leiknes, T.O. Oxidation of Refractory Benzothiazoles with PMS/CuFe₂O₄: Kinetics and Transformation Intermediates. *Environ. Sci. Technol.* **2016**, *50*, 564–5073. [[CrossRef](#)] [[PubMed](#)]
12. Sun, M.; Zhang, Y.; Liu, H.H.; Zhang, F.; Wang, S. Room-temperature air oxidation of organic pollutants via electrocatalysis by nanoscaled Co-CoO on graphite felt anode. *Environ. Int.* **2019**, *131*, 104977. [[CrossRef](#)] [[PubMed](#)]
13. Liu, J.; Zhong, S.; Song, Y.; Wang, B.; Zhang, F. Degradation of tetracycline hydrochloride by electro-activated persulfate oxidation. *J. Electroanal. Chem.* **2018**, *809*, 74–79. [[CrossRef](#)]
14. Wang, J.; Wang, S. Removal of pharmaceuticals and personal care products (PPCPs) from wastewater: A review. *J. Environ. Manag.* **2016**, *182*, 620–640. [[CrossRef](#)] [[PubMed](#)]
15. Zhao, R.; Ma, T.; Zhao, S.; Rong, H. Uniform and stable immobilization of metal-organic frameworks into chitosan matrix for enhanced tetracycline removal from water. *Chem. Eng. J.* **2020**, *382*. [[CrossRef](#)]
16. Zhu, G.; Sun, Q.; Wang, C.; Yang, Z.; Xue, Q. Removal of Sulfamethoxazole, Sulfathiazole and Sulfamethazine in their Mixed Solution by UV/H₂O₂ Process. *Int. J. Environ. Res. Public Health* **2019**, *16*, 1797. [[CrossRef](#)]
17. Ling, C.; Yue, C.; Yuan, R.; Qiu, J.; Liu, F.Q.; Zhu, J.J. Enhanced removal of sulfamethoxazole by an overcomposite of TiO₂ nanocrystals in situ wrapped-Bi₂O₄ microrods under simulated solar irradiation. *Chem. Eng. J.* **2020**, *384*, 123278. [[CrossRef](#)]
18. Chen, C.; Liu, L.; Li, Y.; Li, W.; Zhou, L. Insight into heterogeneous catalytic degradation of sulfamethazine by peroxydisulfate activated with CuCo₂O₄ derived from bimetallic oxalate. *Chem. Eng. J.* **2020**, *384*, 123257. [[CrossRef](#)]
19. Cheng, M.; Liu, Y.; Huang, D.; Lai, C.; Zeng, G.; Huang, J.; Xiong, W. Prussian blue analogue derived magnetic Cu-Fe oxide as a recyclable photo-Fenton catalyst for the efficient removal of sulfamethazine at near neutral pH values. *Chem. Eng. J.* **2019**, *362*, 865–876. [[CrossRef](#)]
20. Liu, X.; Huang, F.; Yu, Y.; Jiang, Y.; Zhao, K.; He, Y.; Zhang, Y. Determination and toxicity evaluation of the generated byproducts from sulfamethazine degradation during catalytic oxidation process. *Chemosphere* **2019**, *226*, 103–109. [[CrossRef](#)]
21. Zbair, M.; Ahsaine, H.A.; Anfar, Z. Porous carbon by microwave assisted pyrolysis: An effective and low-cost adsorbent for sulfamethoxazole adsorption and optimization using response surface methodology. *J. Clean Prod.* **2018**, *202*, 571–581. [[CrossRef](#)]
22. Lawal, I.A.; Lawal, M.M.; Akpotu, S.O.; Moodley, B. Theoretical and experimental adsorption studies of sulfamethoxazole and ketoprofen on synthesized ionic liquids modified CNTs. *Ecotox. Environ. Safe.* **2018**, *161*, 542–552. [[CrossRef](#)] [[PubMed](#)]
23. Prasannamedha, G.; Kumar, P.S. A review on contamination and removal of sulfamethoxazole from aqueous solution using cleaner techniques: Present and future perspective. *J. Clean Prod.* **2020**, *250*, 119553. [[CrossRef](#)]
24. Heo, J.; Yoon, Y.; Lee, G.; Kim, Y.; Park, C.M. Enhanced adsorption of bisphenol A and sulfamethoxazole by a novel magnetic CuZnFe₂O₄-biochar composite. *Bioresour. Technol.* **2019**, *281*, 179–187. [[CrossRef](#)]

25. Zhang, R.; Zheng, X.; Chen, B.; Ma, J.; Niu, X.; Zhou, S. Enhanced adsorption of sulfamethoxazole from aqueous solution by Fe-impregnated graphited biochar. *J. Clean Prod.* **2020**, *256*, 120662. [[CrossRef](#)]
26. Li, S.; Wang, F.; Pan, W.; Yang, X.; Gao, Q.; Sun, W.; Ni, J. Molecular insights into the effects of Cu(II) on sulfamethoxazole and 17 β -estradiol adsorption by carbon nanotubes/CoFe₂O₄ composites. *Chem. Eng. J.* **2019**, *373*, 995–1002. [[CrossRef](#)]
27. Ogunleye, D.T.; Akpotu, S.O.; Moodley, B. Adsorption of sulfamethoxazole and reactive blue 19 using graphene oxide modified with imidazolium based ionic liquid. *Environ. Technol. Innov.* **2020**, *17*, 100616. [[CrossRef](#)]
28. Rostamian, R.; Behnejad, H. A comparative adsorption study of sulfamethoxazole onto graphene and graphene oxide nanosheets through equilibrium, kinetic and thermodynamic modeling. *Process Saf. Environ. Protect.* **2016**, *102*, 20–29. [[CrossRef](#)]
29. Yu, K.; Ahmed, I.; Won, D.-I.; Lee, W.I.; Ahn, W.-S. Highly efficient adsorptive removal of sulfamethoxazole from aqueous solutions by porphyrinic MOF-525 and MOF-545. *Chemosphere* **2020**, *250*, 126133. [[CrossRef](#)]
30. Qiu, H.; Ling, C.; Yuan, R.; Liu, F.; Li, A. Bridging effects behind the coadsorption of copper and sulfamethoxazole by a polyamine-modified resin. *Chem. Eng. J.* **2019**, *362*, 422–429. [[CrossRef](#)]
31. Zheng, M.; Han, Y.; Xu, C.; Zhang, Z.; Han, H. Selective adsorption and bioavailability relevance of the cyclic organics in anaerobic pretreated coal pyrolysis wastewater by lignite activated coke. *Sci. Total Environ.* **2019**, *653*, 64–73. [[CrossRef](#)] [[PubMed](#)]
32. Li, Z.; Wu, L.; Liu, H.; Lan, H.; Qu, J. Improvement of aqueous mercury adsorption on activated coke by thiol-functionalization. *Chem. Eng. J.* **2013**, *228*, 925–934. [[CrossRef](#)]
33. Chen, Y.; Zhang, X.; Liu, Q.; Wang, X.; Zhang, Z. Facile and economical synthesis of porous activated semi-cookes for highly efficient and fast removal of microcystin-LR. *J. Hazard. Mater.* **2015**, *299*, 325–332. [[CrossRef](#)] [[PubMed](#)]
34. Wu, L.; Du, C.; He, H.; Yang, Z.; Li, H. Effective adsorption of diclofenac sodium from neutral aqueous solution by low-cost lignite activated cokes. *J. Hazard. Mater.* **2020**, *384*, 121284. [[CrossRef](#)]
35. Zhuang, S.; Liu, Y.; Wang, J. Covalent organic frameworks as efficient adsorbent for sulfamerazine removal from aqueous solution. *J. Hazard. Mater.* **2020**, *383*, 121126. [[CrossRef](#)]
36. Chowdhury, S.; Saha, P.D. Batch and continuous (fixed-bed column) biosorption of Cu (II) by Tamarindus indica fruit shell. *Korean J. Chem. Eng.* **2013**, *30*, 369–378. [[CrossRef](#)]
37. Ahmad, A.A.; Hameed, B.H. Fixed-bed adsorption of reactive azo dye onto granular activated carbon prepared from waste. *J. Hazard. Mater.* **2010**, *175*, 298–303. [[CrossRef](#)]
38. Chen, K.L.; Liu, L.C.; Chen, W.R. Adsorption of sulfamethoxazole and sulfapyridine antibiotics in high organic content soils. *Environ. Pollut.* **2017**, *231 Pt 1*, 1163–1171. [[CrossRef](#)]
39. Bhadra, B.N.; Seo, P.W.; Jhung, S.H. Adsorption of diclofenac sodium from water using oxidized activated carbon. *Chem. Eng. J.* **2016**, *301*, 27–34. [[CrossRef](#)]
40. Li, Y.; Liu, S.; Wang, C.; Ying, Z.; Huo, M.; Yang, W. Effective column adsorption of triclosan from pure water and wastewater treatment plant effluent by using magnetic porous reduced graphene oxide. *J. Hazard. Mater.* **2020**, *386*, 121942. [[CrossRef](#)]
41. Nithya, K.; Sathish, A.; Kumar, P.S. Packed bed column optimization and modeling studies for removal of chromium ions using chemically modified Lantana camara adsorbent. *Process Saf. Environ. Protect.* **2020**, *33*, 101069. [[CrossRef](#)]
42. Alardhi, S.M.; Albayati, T.M.; Alrubaye, J.M. Adsorption of the methyl green dye pollutant from aqueous solution using mesoporous materials MCM-41 in a fixed-bed column. *Heliyon* **2020**, *6*, e03253. [[CrossRef](#)] [[PubMed](#)]
43. Bo, S.; Luo, J.; An, Q.; Xiao, Z.; Wang, H.; Cai, W.; Li, Z. Efficiently selective adsorption of Pb(II) with functionalized alginate-based adsorbent in batch/column systems: Mechanism and application simulation. *J. Clean Prod.* **2020**, *250*, 119585. [[CrossRef](#)]
44. Weber, W.J.J.; Liu, K.T. Determination of mass transport parameters for fixed-bed. *Chem. Eng. Commun.* **1980**, *6*, 49–60. [[CrossRef](#)]

45. Zheng, M.; Hu, H.; Ye, Z.; Huang, Q.; Chen, X. Adsorption desulfurization performance and adsorption-diffusion study of B₂O₃ modified Ag-CeOx/TiO₂-SiO₂. *J. Hazard. Mater.* **2019**, *362*, 424–435. [[CrossRef](#)]
46. Yu, J.; Yang, F.C.; Hung, W.N.; Liu, C.L.; Yang, M.; Lin, T.F. Prediction of powdered activated carbon doses for 2-MIB removal in drinking water treatment using a simplified HSDM approach. *Chemosphere* **2016**, *156*, 374–382. [[CrossRef](#)]



© 2020 by the authors. Licensee MDPI, Basel, Switzerland. This article is an open access article distributed under the terms and conditions of the Creative Commons Attribution (CC BY) license (<http://creativecommons.org/licenses/by/4.0/>).